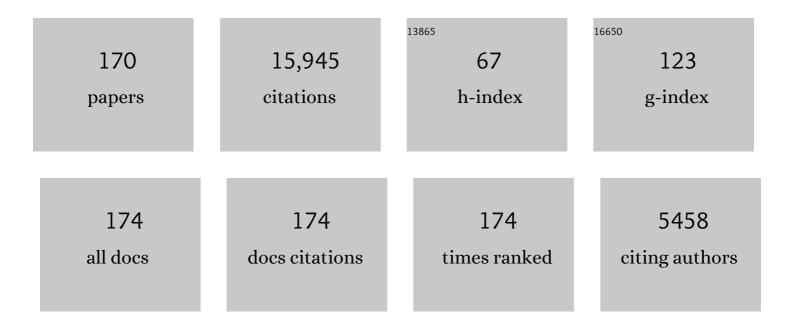
Christoph A Heinrich

List of Publications by Year in descending order

Source: https://exaly.com/author-pdf/401257/publications.pdf Version: 2024-02-01



#	Article	IF	CITATIONS
1	The system H2O–NaCl. Part I: Correlation formulae for phase relations in temperature–pressure–composition space from 0 to 1000°C, 0 to 5000bar, and 0 to 1 XNaCl. Geochimica Et Cosmochimica Acta, 2007, 71, 4880-4901.	3.9	586
2	Quantitative multi-element analysis of minerals, fluid and melt inclusions by laser-ablation inductively-coupled-plasma mass-spectrometry. Geochimica Et Cosmochimica Acta, 2003, 67, 3473-3497.	3.9	484
3	Metal fractionation between magmatic brine and vapor, determined by microanalysis of fluid inclusions. Geology, 1999, 27, 755.	4.4	430
4	Gold concentrations of magmatic brines and the metal budget of porphyry copper deposits. Nature, 1999, 399, 676-679.	27.8	396
5	Capabilities of an Argon Fluoride 193 nm Excimer Laser for Laser Ablation Inductively Coupled Plasma Mass Spectometry Microanalysis of Geological Materials. Journal of Analytical Atomic Spectrometry, 1997, 12, 939-944.	3.0	386
6	The chemistry of hydrothermal tin(-tungsten) ore deposition. Economic Geology, 1990, 85, 457-481.	3.8	354
7	Enhanced sensitivity in laser ablation-ICP mass spectrometry using helium-argon mixtures as aerosol carrier. Journal of Analytical Atomic Spectrometry, 1999, 14, 1363-1368.	3.0	339
8	Special Paper: The Composition of Magmatic-Hydrothermal Fluids in Barren and Mineralized Intrusions. Economic Geology, 2008, 103, 877-908.	3.8	327
9	Formation of a Magmatic-Hydrothermal Ore Deposit: Insights with LA-ICP-MS Analysis of Fluid Inclusions. Science, 1998, 279, 2091-2094.	12.6	323
10	The physical and chemical evolution of low-salinity magmatic fluids at the porphyry to epithermal transition: a thermodynamic study. Mineralium Deposita, 2005, 39, 864-889.	4.1	319
11	Quantitative analysis of major, minor and trace elements in fluid inclusions using laser ablation–inductively coupled plasmamass spectrometry. Journal of Analytical Atomic Spectrometry, 1998, 13, 263-270.	3.0	285
12	Magmatic vapor contraction and the transport of gold from the porphyry environment to epithermal ore deposits. Geology, 2004, 32, 761.	4.4	275
13	Magmatic-hydrothermal evolution in a fractionating granite: a microchemical study of the sn-w-f-mineralized mole granite (Australia). Geochimica Et Cosmochimica Acta, 2000, 64, 3373-3393.	3.9	267
14	Copper deposition by fluid cooling in intrusion-centered systems: New insights from the Bingham porphyry ore deposit, Utah. Geology, 2004, 32, 217.	4.4	267
15	Fluid and source magma evolution of the Questa porphyry Mo deposit, New Mexico, USA. Mineralium Deposita, 2008, 43, 533-552.	4.1	265
16	Copper deposition during quartz dissolution by cooling magmatic–hydrothermal fluids: The Bingham porphyry. Earth and Planetary Science Letters, 2005, 235, 229-243.	4.4	260
17	Hydrothermal Evolution of the El Teniente Deposit, Chile: Porphyry Cu-Mo Ore Deposition from Low-Salinity Magmatic Fluids. Economic Geology, 2007, 102, 1021-1045.	3.8	257
18	Porphyry-Copper Ore Shells Form at Stable Pressure-Temperature Fronts Within Dynamic Fluid Plumes. Science, 2012, 338, 1613-1616.	12.6	253

#	Article	IF	CITATIONS
19	Segregation of ore metals between magmatic brine and vapor; a fluid inclusion study using PIXE microanalysis. Economic Geology, 1992, 87, 1566-1583.	3.8	251
20	Magma evolution and the formation of porphyry Cu?Au ore fluids: evidence from silicate and sulfide melt inclusions. Mineralium Deposita, 2005, 39, 845-863.	4.1	220
21	Kyanite-eclogite to amphibolite fades evolution of hydrous mafic and pelitic rocks, Adula nappe, Central Alps. Contributions To Mineralogy and Petrology, 1982, 81, 30-38.	3.1	218
22	Magmatic-to-hydrothermal crystallization in the W–Sn mineralized Mole Granite (NSW, Australia). Chemical Geology, 2005, 220, 191-213.	3.3	215
23	Trace elements in magnetite from massive iron oxide-apatite deposits indicate a combined formation by igneous and magmatic-hydrothermal processes. Geochimica Et Cosmochimica Acta, 2015, 171, 15-38.	3.9	203
24	Comparison of the ablation behaviour of 266 nm Nd:YAG and 193 nm ArF excimer lasers for LA-ICP-MS analysis. Journal of Analytical Atomic Spectrometry, 1999, 14, 1369-1374.	3.0	192
25	Major to trace element analysis of melt inclusions by laser-ablation ICP-MS: methods of quantification. Chemical Geology, 2002, 183, 63-86.	3.3	190
26	The Bingham Canyon Porphyry Cu-Mo-Au Deposit. III. Zoned Copper-Gold Ore Deposition by Magmatic Vapor Expansion. Economic Geology, 2010, 105, 91-118.	3.8	187
27	Compositions of magmatic hydrothermal fluids determined by LA-ICP-MS of fluid inclusions from the porphyry copper–molybdenum deposit at Butte, MT. Chemical Geology, 2004, 210, 173-199.	3.3	184
28	Eclogite Facies Regional Metamorphism of Hydrous Mafic Rocks in the Central Alpine Adula Nappe. Journal of Petrology, 1986, 27, 123-154.	2.8	182
29	Causes for Large-Scale Metal Zonation around Mineralized Plutons: Fluid Inclusion LA-ICP-MS Evidence from the Mole Granite, Australia. Economic Geology, 2000, 95, 1563-1581.	3.8	179
30	Thermodynamic predictions of the hydrothermal chemistry of arsenic, and their significance for the paragenetic sequence of some cassiterite-arsenopyrite-base metal sulfide deposits. Economic Geology, 1986, 81, 511-529.	3.8	175
31	The magma and metal source of giant porphyry-type ore deposits, based on lead isotope microanalysis of individual fluid inclusions. Earth and Planetary Science Letters, 2010, 296, 267-277.	4.4	172
32	Fluid-Fluid Interactions in Magmatic-Hydrothermal Ore Formation. Reviews in Mineralogy and Geochemistry, 2007, 65, 363-387.	4.8	165
33	Zircon crystallization and the lifetimes of ore-forming magmatic-hydrothermal systems. Geology, 2011, 39, 731-734.	4.4	163
34	3: Geochronology and geodynamics of Late Cretaceous magmatism and Cu–Au mineralization in the Panagyurishte region of the Apuseni–Banat–Timok–Srednogorie belt, Bulgaria. Ore Geology Reviews, 2005, 27, 95-126.	2.7	161
35	The Origin of Cu/Au Ratios in Porphyry-Type Ore Deposits. Science, 2002, 296, 1844-1846.	12.6	157
36	Fluid-rock interaction is decisive for the formation of tungsten deposits. Geology, 2017, 45, 579-582.	4.4	155

3

#	Article	IF	CITATIONS
37	The role of sulfur in the formation of magmatic–hydrothermal copper–gold deposits. Earth and Planetary Science Letters, 2009, 282, 323-328.	4.4	154
38	Sediment-Hosted Gold Deposits in Guizhou, China: Products of Wall-Rock Sulfidation by Deep Crustal Fluids. Economic Geology, 2009, 104, 73-93.	3.8	147
39	Copper partitioning in a melt–vapor–brine–magnetite–pyrrhotite assemblage. Geochimica Et Cosmochimica Acta, 2006, 70, 5583-5600.	3.9	146
40	Evolution of Magmatic Vapor to Gold-Rich Epithermal Liquid: The Porphyry to Epithermal Transition at Nevados de Famatina, Northwest Argentina. Economic Geology, 2009, 104, 449-477.	3.8	146
41	Magnetite solubility and iron transport in magmatic-hydrothermal environments. Geochimica Et Cosmochimica Acta, 2004, 68, 4905-4914.	3.9	144
42	From a long-lived upper-crustal magma chamber to rapid porphyry copper emplacement: Reading the geochemistry of zircon crystals at Bajo de la Alumbrera (NW Argentina). Earth and Planetary Science Letters, 2016, 450, 120-131.	4.4	137
43	Separation of Molybdenum and Copper in Porphyry Deposits: The Roles of Sulfur, Redox, and pH in Ore Mineral Deposition at Bingham Canyon. Economic Geology, 2012, 107, 333-356.	3.8	125
44	The Structure and Dynamics of Mid-Ocean Ridge Hydrothermal Systems. Science, 2008, 321, 1825-1828.	12.6	124
45	Sensitivity enhancement in laser ablation ICP-MS using small amounts of hydrogen in the carrier gas. Journal of Analytical Atomic Spectrometry, 2007, 22, 1488.	3.0	118
46	Alkali metals control the release of gold from volatile-rich magmas. Earth and Planetary Science Letters, 2010, 297, 50-56.	4.4	116
47	2: Hydrothermal ore deposits related to post-orogenic extensional magmatism and core complex formation: The Rhodope Massif of Bulgaria and Greece. Ore Geology Reviews, 2005, 27, 53-89.	2.7	115
48	Cu – Au – Pb – Zn – Ag metallogeny of the Alpine – Balkan – Carpathian – Dinaride geodynamic province. Mineralium Deposita, 2002, 37, 533-540.	4.1	111
49	Gold partitioning in melt-vapor-brine systems. Geochimica Et Cosmochimica Acta, 2005, 69, 3321-3335.	3.9	110
50	The Evolution of a Porphyry Cu-Au Deposit, Based on LA-ICP-MS Analysis of Fluid Inclusions: Bajo de la Alumbrera, Argentina. Economic Geology, 2002, 97, 1889-1920.	3.8	105
51	Accurate quantification of melt inclusion chemistry by LA-ICPMS: a comparison with EMP and SIMS and advantages and possible limitations of these methods. Lithos, 2004, 78, 333-361.	1.4	103
52	Microanalysis of S, Cl, and Br in fluid inclusions by LA–ICP-MS. Chemical Geology, 2011, 284, 35-35.	3.3	102
53	A spectrophotometric study of aqueous iron (II) chloride complexing from 25 to 200°C. Geochimica Et Cosmochimica Acta, 1990, 54, 2207-2221.	3.9	97
54	Diffusive reequilibration of quartz-hosted silicate melt and fluid inclusions: Are all metal concentrations unmodified?. Geochimica Et Cosmochimica Acta, 2009, 73, 3013-3027.	3.9	97

#	Article	IF	CITATIONS
55	The partitioning behavior of As and Au in S-free and S-bearing magmatic assemblages. Geochimica Et Cosmochimica Acta, 2007, 71, 1764-1782.	3.9	89
56	Numerical simulation of multi-phase fluid flow in structurally complex reservoirs. Geological Society Special Publication, 2007, 292, 405-429.	1.3	88
57	Determination of sulfur in fluid inclusions by laser ablation ICP-MS. Journal of Analytical Atomic Spectrometry, 2008, 23, 1581.	3.0	83
58	Phase separation, brine formation, and salinity variation at Black Smoker hydrothermal systems. Journal of Geophysical Research, 2009, 114, .	3.3	83
59	Tectonic, magmatic, and metallogenic evolution of the Late Cretaceous arc in the Carpathianâ€Balkan orogen. Tectonics, 2015, 34, 1813-1836.	2.8	83
60	Magmatic-to-hydrothermal crystallization in the W–Sn mineralized Mole Granite (NSW, Australia). Chemical Geology, 2005, 220, 215-235.	3.3	82
61	Direct Analysis of Ore-Precipitating Fluids: Combined IR Microscopy and LA-ICP-MS Study of Fluid Inclusions in Opaque Ore Minerals. Economic Geology, 2010, 105, 351-373.	3.8	81
62	Chemistry of low-temperature hydrothermal gold, platinum, and palladium (+ or - uranium) mineralization at Coronation Hill, Northern Territory, Australia. Economic Geology, 1994, 89, 1053-1073.	3.8	79
63	Fluid mixing forms basement-hosted Pb-Zn deposits: Insight from metal and halogen geochemistry of individual fluid inclusions. Geology, 2013, 41, 679-682.	4.4	78
64	The relation between Cu/Au ratio and formation depth of porphyry-style Cu–Au ± Mo deposits. Mineralium Deposita, 2010, 45, 11-21.	4.1	76
65	Fluid and mass transfer during metabasalt alteration and copper mineralization at Mount Isa, Australia. Economic Geology, 1995, 90, 705-730.	3.8	75
66	Multiphase Thermohaline Convection in the Earth's Crust: I. A New Finite Element – Finite Volume Solution Technique Combined With a New Equation of State for NaCl–H2O. Transport in Porous Media, 2006, 63, 399-434.	2.6	73
67	Direct liquid ablation: a new calibration strategy for laser ablation-ICP-MS microanalysis of solids and liquids. Fresenius' Journal of Analytical Chemistry, 1997, 359, 390-393.	1.5	70
68	From andesitic volcanism to the formation of a porphyry Cu-Au mineralizing magma chamber: the Farallųn Negro Volcanic Complex, northwestern Argentina. Journal of Volcanology and Geothermal Research, 2004, 136, 1-30.	2.1	69
69	Hydrodynamic modeling of magmatic–hydrothermal activity at submarine arc volcanoes, with implications for ore formation. Earth and Planetary Science Letters, 2014, 404, 307-318.	4.4	67
70	Trace elements in fluid inclusions of sediment-hosted gold deposits indicate a magmatic-hydrothermal origin of the Carlin ore trend. Geology, 2016, 44, 1015-1018.	4.4	64
71	Magma Evolution Leading to Porphyry Au-Cu Mineralization at the Ok Tedi Deposit, Papua New Guinea: Trace Element Geochemistry and High-Precision Geochronology of Igneous Zircon. Economic Geology, 2018, 113, 39-61.	3.8	64
72	Quantitative PIXE microanalysis of fluid inclusions based on a layered yield model. Nuclear Instruments & Methods in Physics Research B, 1991, 54, 292-297.	1.4	63

#	Article	IF	CITATIONS
73	The dynamics of mid-ocean ridge hydrothermal systems: Splitting plumes and fluctuating vent temperatures. Earth and Planetary Science Letters, 2006, 245, 218-231.	4.4	63
74	Magmatic Fluids in the Breccia-Hosted Epithermal Au-Ag Deposit of Rosia Montana, Romania. Economic Geology, 2006, 101, 923-954.	3.8	63
75	Quadrupole mass spectrometry and optical emission spectroscopy: detection capabilities and representative sampling of short transient signals from laser-ablation. Journal of Analytical Atomic Spectrometry, 2000, 15, 1149-1155.	3.0	62
76	Adakite-like and Normal Arc Magmas: Distinct Fractionation Paths in the East Serbian Segment of the Balkan–Carpathian Arc. Journal of Petrology, 2013, 54, 421-451.	2.8	59
77	Witwatersrand gold deposits formed by volcanicÂrain, anoxic rivers and Archaean life. Nature Geoscience, 2015, 8, 206-209.	12.9	57
78	Stable isotope (B, H, O) and mineral-chemistry constraints on the magmatic to hydrothermal evolution of the VarutrÃ s k rare-element pegmatite (Northern Sweden). Chemical Geology, 2016, 421, 1-16.	3.3	56
79	A fluid inclusion and stable isotope study of synmetamorphic copper ore formation at Mount Isa, Australia. Economic Geology, 1989, 84, 529-550.	3.8	55
80	Chemical mass transfer modelling of ore-forming hydrothermal systems: current practise and problems. Ore Geology Reviews, 1996, 10, 319-338.	2.7	55
81	Fluid evolution in zoned Cordilleran polymetallic veins — Insights from microthermometry and LA-ICP-MS of fluid inclusions. Chemical Geology, 2011, 281, 293-304.	3.3	55
82	Melt and Fluid Inclusions in Hydrothermal Veins: The Magmatic to Hydrothermal Evolution of the Elatsite Porphyry Cu-Au Deposit, Bulgaria. Economic Geology, 2014, 109, 1359-1381.	3.8	55
83	Contrasting hydrological processes of meteoric water incursion during magmatic–hydrothermal ore deposition: An oxygen isotope study by ion microprobe. Earth and Planetary Science Letters, 2016, 451, 263-271.	4.4	55
84	Laser-ablation ICP-MS analysis of silicate and sulfide melt inclusions in an andesitic complex I: analytical approach and data evaluation. Contributions To Mineralogy and Petrology, 2004, 147, 385-396.	3.1	54
85	Zircon petrochronological evidence for a plutonic-volcanic connection in porphyry copper deposits. Geology, 2017, 45, 623-626.	4.4	52
86	Br/Cl geochemistry of hydrothermal brines associated with Proterozoic metasediment-hosted copper mineralization at Mount Isa, northern Australia. Geochimica Et Cosmochimica Acta, 1993, 57, 2991-3000.	3.9	51
87	PIXE microanalysis of fluid inclusions and its application to study ore metal segregation between magmatic brine and vapor. Nuclear Instruments & Methods in Physics Research B, 1993, 77, 463-471.	1.4	50
88	A fluid inclusion reconnaissance study of the Huanuni tin deposit (Bolivia), using LA-ICP-MS micro-analysis. Mineralium Deposita, 2001, 36, 680-688.	4.1	49
89	The Bingham Canyon Porphyry Cu-Mo-Au Deposit. II. Vein Geometry and Ore Shell Formation by Pressure-Driven Rock Extension. Economic Geology, 2010, 105, 69-90.	3.8	48
90	Selective copper diffusion into quartz-hosted vapor inclusions: Evidence from other host minerals, driving forces, and consequences for Cu–Au ore formation. Geochimica Et Cosmochimica Acta, 2013, 113, 60-69.	3.9	48

#	Article	IF	CITATIONS
91	Internally consistent thermodynamic data for aqueous species in the system Na–K–Al–Si–O–H–Cl. Geochimica Et Cosmochimica Acta, 2016, 187, 41-78.	3.9	47
92	40 Ar/ 39 Ar geochronology of copper mineralization and regional alteration, Mount Isa, Australia. Economic Geology, 1999, 94, 23-36.	3.8	46
93	Fluid Fluid Interactions in the Earth's Lithosphere. Reviews in Mineralogy and Geochemistry, 2007, 65, 1-13.	4.8	46
94	Shale basins, sulfur-deficient ore brines and the formation of exhalative base metal deposits. Chemical Geology, 2008, 247, 195-207.	3.3	45
95	Time evolution of a rifted continental arc: Integrated ID-TIMS and LA-ICPMS study of magmatic zircons from the Eastern Srednogorie, Bulgaria. Lithos, 2012, 154, 53-67.	1.4	45
96	Magmatic salt melt and vapor: Extreme fluids forming porphyry gold deposits in shallow subvolcanic settings. Geology, 2014, 42, 495-498.	4.4	44
97	Gold concentrations in metamorphic fluids: A LA-ICPMS study of fluid inclusions from the Alpine orogenic belt. Chemical Geology, 2014, 385, 70-83.	3.3	44
98	Quantification of transient signals in multiple collector inductively coupled plasma mass spectrometry: accurate lead isotope ratio determination by laser ablation of individual fluid inclusions. Journal of Analytical Atomic Spectrometry, 2011, 26, 475-492.	3.0	43
99	The Elatsite porphyry copper deposit in the Panagyurishte ore district, Srednogorie zone, Bulgaria: U-Pb zircon geochronology and isotope-geochemical investigations of magmatism and ore genesis. Geological Society Special Publication, 2002, 204, 119-135.	1.3	42
100	The partitioning behavior of silver in a vapor–brine–rhyolite melt assemblage. Geochimica Et Cosmochimica Acta, 2008, 72, 1638-1659.	3.9	42
101	Application of low-temperature microthermometric data for interpreting multicomponent fluid inclusion compositions. Earth-Science Reviews, 2016, 159, 14-35.	9.1	41
102	Mechanisms and patterns of magmatic fluid transport in cooling hydrous intrusions. Earth and Planetary Science Letters, 2020, 535, 116111.	4.4	41
103	100th Anniversary Special Paper: Vapor Transport of Metals and the Formation of Magmatic-Hydrothermal Ore Deposits. Economic Geology, 2005, 100, 1287-1312.	3.8	40
104	Microanalysis of ore-forming fluids using the scanning proton microprobe. Nuclear Instruments & Methods in Physics Research B, 1995, 104, 182-190.	1.4	39
105	Post-Orogenic Extension and Hydrothermal Ore Formation: High-Precision Geochronology of the Central Rhodopian Metamorphic Core Complex (Bulgaria-Greece). Economic Geology, 2013, 108, 691-718.	3.8	39
106	Laser-ablation ICP-MS analysis of silicate and sulfide melt inclusions in an andesitic complex II: evidence for magma mixing and magma chamber evolution. Contributions To Mineralogy and Petrology, 2004, 147, 397-412.	3.1	38
107	Major and trace-element composition and pressure–temperature evolution of rock-buffered fluids in low-grade accretionary-wedge metasediments, Central Alps. Contributions To Mineralogy and Petrology, 2013, 165, 981-1008.	3.1	38
108	On the dynamics of NaCl-H2O fluid convection in the Earth's crust. Journal of Geophysical Research, 2005, 110, .	3.3	37

#	Article	IF	CITATIONS
109	Multiphase Thermohaline Convection in the Earth's Crust: II. Benchmarking and Application of a Finite Element – Finite Volume Solution Technique with a NaCl–H2O Equation of State. Transport in Porous Media, 2006, 63, 435-461.	2.6	37
110	Highâ€resolution threeâ€dimensional simulations of midâ€ocean ridge hydrothermal systems. Journal of Geophysical Research, 2009, 114, .	3.3	37
111	Experimental determination of Au solubility in rhyolite melt and magnetite: Constraints on magmatic Au budgets. American Mineralogist, 2003, 88, 1644-1651.	1.9	35
112	Fluids and Ore Formation in the Earth's Crust. , 2014, , 1-28.		35
113	Microanalysis of Fluid Inclusions in Crustal Hydrothermal Systems using Laser Ablation Methods. Elements, 2016, 12, 323-328.	0.5	35
114	Is the Mount Isa copper deposit the product of forced brine convection in the footwall of a major reverse fault?. Geology, 2004, 32, 357.	4.4	35
115	Physical, chemical and mineralogical evolution of the Tolhuaca geothermal system, southern Andes, Chile: Insights into the interplay between hydrothermal alteration and brittle deformation. Journal of Volcanology and Geothermal Research, 2016, 324, 88-104.	2.1	34
116	Source Plutons Driving Porphyry Copper Ore Formation: Combining Geomagnetic Data, Thermal Constraints, and Chemical Mass Balance to Quantify the Magma Chamber Beneath the Bingham Canyon Deposit. Economic Geology, 2013, 108, 605-624.	3.8	33
117	Combining trace-element compositions, U–Pb geochronology and Hf isotopes in zircons to unravel complex calcalkaline magma chambers in the Upper Cretaceous Srednogorie zone (Bulgaria). Lithos, 2008, 104, 405-427.	1.4	32
118	U–Pb dating, Hf-isotope characteristics and trace-REE-patterns of zircons from Medet porphyry copper deposit, Bulgaria: implications for timing, duration and sources of ore-bearing magmatism. Mineralogy and Petrology, 2009, 96, 19-41.	1.1	31
119	Chemical evolution of metamorphic fluids in the Central Alps, Switzerland: insight from <scp>LA</scp> â€ <scp>ICPMS</scp> analysis of fluid inclusions. Geofluids, 2016, 16, 877-908.	0.7	31
120	LA-ICP-MS analysis of fluid inclusions: contamination effects challenging micro-analysis of elements close to their detection limit. Journal of Analytical Atomic Spectrometry, 2017, 32, 1052-1063.	3.0	31
121	Chlorine partitioning between granitic melt and H2O-CO2-NaCl fluids in the Earth's upper crust and implications for magmatic-hydrothermal ore genesis. Geochimica Et Cosmochimica Acta, 2019, 261, 171-190.	3.9	30
122	A magmatic source of hydrothermal sulfur for the Prominent Hill deposit and associated prospects in the Olympic iron oxide copper-gold (IOCG) province of South Australia. Ore Geology Reviews, 2017, 89, 1058-1090.	2.7	27
123	Fluid-Flow Patterns at Brothers Volcano, Southern Kermadec Arc: Insights from Geologically Constrained Numerical Simulations. Economic Geology, 2012, 107, 1595-1611.	3.8	26
124	Tethyan mantle metasomatism creates subduction geochemical signatures in non-arc Cu–Au–Te mineralizing magmas, Apuseni Mountains (Romania). Earth and Planetary Science Letters, 2013, 366, 122-136.	4.4	26
125	Sulfur isotope systematics of copper ore formation at Mount Isa, Australia. Economic Geology, 1989, 84, 1614-1626.	3.8	25
126	A palaeomagnetic study of hydrothermal activity and uranium mineralization at Mt Painter, South Australia. Australian Journal of Earth Sciences, 1993, 40, 87-101.	1.0	25

#	Article	IF	CITATIONS
127	Gold precipitation by fluid mixing in bedding-parallel fractures near carbonaceous slates at the Cosmopolitan Howley gold deposit, northern Australia. Economic Geology, 1995, 90, 2123-2142.	3.8	25
128	The formation of economic porphyry copper (-gold) deposits: constraints from microanalysis of fluid and melt inclusions. Geological Society Special Publication, 2005, 248, 247-263.	1.3	24
129	The Porphyry Cu-(Mo-Au) Deposit at Altar (Argentina): Tracing Gold Distribution by Vein Mapping and LA-ICP-MS Mineral Analysis. Economic Geology, 2014, 109, 1341-1358.	3.8	24
130	Melt and fluid evolution in an upper-crustal magma reservoir, preserved by inclusions in juvenile clasts from the Kos Plateau Tuff, Aegean Arc, Greece. Geochimica Et Cosmochimica Acta, 2020, 280, 237-262.	3.9	24
131	An evaluation of synthetic fluid inclusions for the purpose of trapping equilibrated, coexisting, immiscible fluid phases at magmatic conditions. American Mineralogist, 2007, 92, 124-138.	1.9	23
132	Origin of Nepheline-normative High-K Ankaramites and the Evolution of Eastern Srednogorie Arc in SE Europe. Journal of Petrology, 2009, 50, 1899-1933.	2.8	23
133	Geochronology, geochemistry and isotope tracing of the Oligocene magmatism of the Buchim–Damjan–Borov Dol ore district: Implications for timing, duration and source of the magmatism. Lithos, 2013, 180-181, 216-233.	1.4	23
134	The optimal windows for seismically-enhanced gold precipitation in the epithermal environment. Ore Geology Reviews, 2016, 79, 463-473.	2.7	23
135	Fluid evolution in a volcanic-hosted epithermal carbonate–base metal–gold vein system: Alto de la Blenda, Farallón Negro, Argentina. Mineralium Deposita, 2016, 51, 873-902.	4.1	23
136	Lithology and Hydrothermal Alteration Control the Distribution of Copper Grade in the Prominent Hill Iron Oxide-Copper-Gold Deposit (Gawler Craton, South Australia). Economic Geology, 2015, 110, 1953-1994.	3.8	23
137	Resolving the timescales of magmatic and hydrothermal processes associated with porphyry deposit formation using zircon U–Pb petrochronology. Geochronology, 2020, 2, 209-230.	2.5	23
138	Heat transport at boiling, near ritical conditions. Geofluids, 2008, 8, 208-215.	0.7	22
139	Hematite Breccia-Hosted Iron Oxide Copper-Gold Deposits Require Magmatic Fluid Components Exposed to Atmospheric Oxidation: Evidence from Prominent Hill, Gawler Craton, South Australia. Economic Geology, 2018, 113, 597-644.	3.8	21
140	Semi-quantitative electron microprobe analysis of fluid inclusion salts from the Mount Isa copper deposit (Queensland, Australia). Geochimica Et Cosmochimica Acta, 1989, 53, 21-28.	3.9	19
141	Three-dimensional geometry, ore distribution and time-integrated mass transfer through the quartz-tourmaline-gold vein network of the Sigma deposit (Abitibi belt, Canada). Geofluids, 2002, 2, 217-232.	0.7	19
142	TEMPERATURE GRADIENTS RECORDED BY FLUID INCLUSIONS AND HYDROTHERMAL ALTERATION AT THE MOUNT CHARLOTTE GOLD DEPOSIT, KALGOORLIE, AUSTRALIA. Canadian Mineralogist, 2004, 42, 1383-1404.	1.0	19
143	Mafic dikes displacing Witwatersrand gold reefs: Evidence against metamorphic-hydrothermal ore formation. Geology, 2009, 37, 607-610.	4.4	19
144	Accurate and precise quantification of major and trace element compositions of calcic–sodic fluid inclusions by combined microthermometry and LA-ICPMS analysis. Chemical Geology, 2012, 334, 144-153.	3.3	19

#	Article	IF	CITATIONS
145	Geodynamics and ore deposit evolution in Europe: Introduction. Ore Geology Reviews, 2005, 27, 5-11.	2.7	17
146	Causes for Large-Scale Metal Zonation around Mineralized Plutons: Fluid Inclusion LA-ICP-MS Evidence from the Mole Granite, Australia. Economic Geology, 2000, 95, 1563-1581.	3.8	17
147	Estimation and testing of standard molar thermodynamic properties of tourmaline end-members using data of natural samples. American Mineralogist, 2000, 85, 78-88.	1.9	16
148	9: Processes of tectonism, magmatism and mineralization: Lessons from Europe. Ore Geology Reviews, 2005, 27, 333-349.	2.7	16
149	GEOCHEMISTRY: How Fast Does Gold Trickle Out of Volcanoes?. Science, 2006, 314, 263-264.	12.6	16
150	Silver Isotopes as a Source and Transport Tracer for Gold: A Reconnaissance Study at the Sheba and New Consort Gold Mines in the Barberton Greenstone Belt, Kaapvaal Craton, South Africaâ~¼. Economic Geology, 2018, 113, 1553-1570.	3.8	16
151	The Serra Pelada Au-Pd-Pt Deposit, Carajas, Brazil: Geochemistry, Mineralogy, and Zoning of Hydrothermal Alteration. Economic Geology, 2014, 109, 1883-1899.	3.8	14
152	Copper partitioning between silicate melts and amphibole: Experimental insight into magma evolution leading to porphyry copper ore formation. Chemical Geology, 2017, 448, 151-163.	3.3	13
153	Fluid inclusion measurements by laser ablation sector-field ICP-MS. Journal of Analytical Atomic Spectrometry, 2014, 29, 1052-1057.	3.0	12
154	Fluid Evolution and Uranium (-Mo-F) Mineralization at the Maureen Deposit (Queensland, Australia): Unconformity-Related Hydrothermal Ore Formation with a Source in the Volcanic Cover Sequence. Economic Geology, 2014, 109, 737-773.	3.8	10
155	Fluid Evolution at the Batu Hijau Porphyry Cu-Au Deposit, Indonesia: Hypogene Sulfide Precipitation from a Single-Phase Aqueous Magmatic Fluid During Chlorite–White-Mica Alteration. Economic Geology, 2022, 117, 979-1012.	3.8	10
156	Ore mineralogy of the Serra Pelada Au-Pd-Pt deposit, Carajás, Brazil and implications for ore-forming processes. Mineralium Deposita, 2016, 51, 781-795.	4.1	9
157	Evolution of the Breccia-Hosted Porphyry Cu-Mo-Au Deposit at Agua Rica, Argentina: Progressive Unroofing of a Magmatic Hydrothermal System. Economic Geology, 2002, 97, 1273-1292.	3.8	9
158	3-1: The Elatsite porphyry Cu–Au deposit, Bulgaria. Ore Geology Reviews, 2005, 27, 128-129.	2.7	8
159	From fluid inclusion microanalysis to large-scale hydrothermal mass transfer in the Earth's interior. Journal of Mineralogical and Petrological Sciences, 2006, 101, 110-117.	0.9	8
160	Fluid Evolution of the Monte Mattoni Mafic Complex, Adamello Batholith, Northern Italy: Insights from Fluid Inclusion Analysis and Thermodynamic Modeling. Journal of Petrology, 2017, 58, 1645-1670.	2.8	8
161	11. Fluid-Fluid Interactions in Magmatic-Hydrothermal Ore Formation. , 2007, , 363-388.		7
162	The influence of water in silicate melt on aluminium excess in plagioclase as a potential hygrometer. Scientific Reports, 2018, 8, 12421.	3.3	7

#	Article	IF	CITATIONS
163	Advantages of a fast-scanning quadrupole for LA-ICP-MS analysis of fluid inclusions. Journal of Analytical Atomic Spectrometry, 2021, 36, 2043-2050.	3.0	6
164	Fluid geochemistry of the Serra Pelada Au-Pd-Pt deposit, CarajÃįs, Brazil: Exceptional metal enrichment caused by deep reaching hydrothermal oxidation. Ore Geology Reviews, 2019, 111, 102991.	2.7	5
165	Evolution from magmatic to hydrothermal activity beneath the Cerro Escorial volcano (NW) Tj ETQq1 1 0.784314	rgBT /Ov 1.4	erlock 10 Tfl
166	Silicate-replacive high sulfidation massive sulfide orebodies in a porphyry Cu-Au system: Bor, Serbia. Mineralium Deposita, 2021, 56, 1423-1448.	4.1	3
167	Geology and Alteration Geochemistry of the Porphyry Cu-Au Deposit at Bajo de la Alumbrera, Argentina. Economic Geology, 2002, 97, 1865-1888.	3.8	2
168	Hydrothermal Systems. , 1992, , 42-100.		0
169	Maria Sch̦nb̾hler receives the 2007 Paul Niggli Medal. Swiss Journal of Geosciences, 2008, 101, 237-238.	1.2	0
170	Waldemar Lindgren Award for 2003 Citation of Werner E. Halter. Economic Geology, 2004, 99, 1819-1820.	3.8	0